A 3.06-Mb interstitial deletion on 12p11.22-12.1 caused brachydactyly type E combined with pectus carinatum

Jia Huang[1,2], Hong-Yan Liu[2], Rong-Rong Wang[3], Hai Xiao[2], Dong Wu[2], Tao Li[2], Ying-Hai Jiang[2], Xue Zhang[1,3]

[1]The Research Center for Medical Genomics, Key Laboratory of Medical Cell Biology, Chinese Ministry of Education, College of Basic Medical Science, China Medical University, Shenyang, Liaoning 110122, China;

[2]Institute of Medical Genetics, Henan Provincial People's Hospital, People's Hospital of Zhengzhou University, School of Clinical Medicine, Henan University, Zhengzhou, Henan 450003, China;

[3]McKusick-Zhang Center for Genetic Medicine, State Key Laboratory of Medical Molecular Biology, Institute of Basic Medical Sciences Chinese Academy of Medical Sciences, School of Basic Medicine Peking Union Medical College, Beijing 100005, China.

Abstract

Background: Brachydactyly, a developmental disorder, refers to shortening of hands/feet due to small or missing metacarpals/metatarsals and/or phalanges. Isolated brachydactyly type E (BDE), characterized by shortened metacarpals and/or metatarsals, consists in a small proportion of patients with Homeobox D13 (*HOXD13*) or parathyroid-hormone-like hormone (*PTHLH*) mutations. BDE is often accompanied by other anomalies that are parts of many congenital syndromes. In this study, we investigated a Chinese family presented with BDE combined with pectus carinatum and short stature.

Methods: A four-generation Chinese family was recruited in June 2016. After informed consent was obtained, venous blood was collected, and genomic DNA was extracted by standard procedures. Whole-exome sequencing was performed to screen pathogenic mutation, array comparative genomic hybridization (Array-CGH) analysis was used to analyze copy number variations, and quantitative real-time polymerase chain reaction (PCR), stride over breakpoint PCR (gap-PCR), and Sanger sequencing were performed to confirm the candidate variation.

Results: A 3.06-Mb deletion (chr12:25473650–28536747) was identified and segregated with the phenotype in this family. The deletion region encompasses 23 annotated genes, one of which is *PTHLH* which has been reported to be causative to the BDE. *PTHLH* is an important regulator of endochondral bone development. The affected individuals showed bilateral, severe, and generalized brachydactyly with short stature, pectus carinatum, and prematurely fusion of epiphyses. The feature of pectus carinatum has not been described in the *PTHLH*-related BDE patients previously.

Conclusions: The haploinsufficiency of *PTHLH* might be responsible for the disease in this family. This study has expanded the knowledge on the phenotypic presentation of *PTHLH* variation.

Keywords: Brachydactyly type E; Parathyroid-hormone-like hormone; Pectus carinatum; Short stature; Copy number variation

Introduction

Brachydactyly (BD) is a developmental disorder, referring to shortening of the hands/feet due to small or missing metacarpals/metatarsals and/or phalange.[1] BD can occur as an isolated malformation or with other anomalies that are parts of many congenital syndromes. According to the patterns of skeletal involvement, isolated BD has been classified into five groups (A–E).[2] The BD type A is characterized by hypoplasia/aplasia of the middle phalanges, type B by hypoplasia/aplasia of the terminal (distal) phalanges, type C is more complex with shortening of multiple phalanges and a relatively normal fourth finger, whereas type D refers to a short distal phalanx of the thumb and type E is characterized by shortening of the metacarpals and/or metatarsals with frequent involvement of the phalanges.[1] Hertzog[3] classified BD type E (BDE) into three distinct types: E1, shortening is limited to the fourth metacarpals and/or metatarsals; E2, shortening is in metacarpals IV and V, and/or metatarsals, including shortening of the distal phalanx of the thumb; and E3, variable combinations of shortened metacarpals without phalangeal involvement. However, this classification does not apply to all syndromes because other phalanges are often involved.

In the isolated BDE, heterozygous mutations in the *HOXD13* have been described,[4,5] and are overlapped

Access this article online

Quick Response Code:

Website: www.cmj.org

DOI: 10.1097/CM9.0000000000000327

Correspondence to: Prof. Xue Zhang, The Research Center for Medical Genomics, Key Laboratory of Medical Cell Biology, Chinese Ministry of Education, College of Basic Medical Science, China Medical University, Shenyang, Liaoning 110122, China
E-Mail: xuezhang@pumc.edu.cn

Chinese Medical Journal 2019;132(14)

Received: 16-05-2019 **Edited by:** Peng Lyu

with BD type D.[4] Most of BDE patients with *HOXD13* mutations had shortening of metacarpal III, sometimes IV and V, and little finger distal phalanx hypoplasia and syndactyly of finger III/IV were frequently observed.[4] Recently, it was shown that heterozygous mutations in *PTHLH* could also lead to BDE2,[6-9] often associated with a feature of short stature, and the phenotypes are variable even within families,[8,9] ranging from moderate shortening of individual metacarpals to shortening of all bones in the hands and/or feet. However, the majority of BDE cases often occur in association with a syndrome. BDE in combination with hypertension was mapped to a region of 12p,[10,11] and phosphodiesterase 3A (*PDE3A*) was identified as the pathogenic gene of this syndrome.[12] BDE may be accompanied with a hormonal resistance syndrome, such as pseudohypoparathyroidism (PHP, OMIM 103580, OMIM 603233, OMIM 612462), in which resistance to parathyroid hormone (PTH) is the most prominent feature, and mutations in G protein alpha stimulating (*GNAS*) being responsible for this disease.[13] Acrodysostosis (ACRDYS1, OMIM 101800) may also be present, which is a skeletal dysplasia characterized by severe generalized BD of hands and feet with short stature, facial abnormalities, obesity, intellectual disability and impaired hearing being frequently observed. Resistance to PTH or thyroid-stimulating hormone (TSH) is one of the important features of ACRDYS1, and mutations in protein kinase A type 1a regulatory subunit (*PRKAR1A*) having been identified to be associated with ACRDYS1.[14] Acrodysostosis without multi-hormonal resistance (ACRDYS2, OMIM 614613) may also occur, which is similar to ACRDYS1 in clinical features apart from the hormonal resistance, and mutations in phosphodiesterase 4D (*PDE4D*) are associated with this disease.[14,15] In addition, BD mental retardation syndrome (BDMR, OMIM 600430), Albright's hereditary osteodystrophy (AHO), tricho-rhino-phalangeal syndrome (TRPS, OMIM 190350, OMIM 150230, OMIM 190351) and Turner syndrome (TS) have been described to have BDE as one of the clinical features.

In this study, we reported a four-generation Chinese pedigree with an unclassified BDE syndrome, presenting with severe generalized BD, pectus carinatum, and short stature. A micro-deletion of 3.06 Mb located on 12p11.22-12.1 was confirmed to be associated with this syndrome.

Methods

Ethical approval

The study was conducted in accordance with the *Declaration of Helsinki* and was approved by the Ethics Committee of Henan Provincial People's Hospital (2018–No. 3). Written informed consent was obtained from all participants.

Participants

A four-generation Chinese family with severe generalized BD, pectus carinatum, and short stature was recruited in June 2016. The pedigree chart is shown in Figure 1. Clinical data and digital photographs of hands and feet were obtained from the patients. Peripheral venous blood (EDTA-K2 anticoagulant) from 17 family members of this family were collected, including nine patients (II3, II6, III5, III8, III10, III11, III12, IV2, and IV5) and eight unaffected individuals (II2, II4, III4, III6, III7, III9, IV1, and IV6). Genomic DNA was extracted from peripheral blood lymphocytes by standard procedures using Qiagen whole blood kit (QIAGEN, Hilden, Germany).

Whole exome sequencing

Whole exome sequencing (WES) was performed on genomic DNA of three affected individuals (III8, III12, and IV2). Exome libraries were prepared using the SureSelect Human All Exon V4 kit (Agilent, Santa Clara, CA, USA) and sequenced using the HiSeq2000 system (Illumina, San Diego, CA, USA). The quality-control metrics (QC) were set to only retain variants in the positions with read depth ≥10, genotype quality ≥20, and alternate allele read ratio ≥0.25. Variations were annotated using UCSC hg19 refGene.txt.gz (http://hgdownload.cse.ucsc.edu/goldenPath/hg19/database/). Genome Analysis Toolkit (Broad Institute, Harvard and MIT, MA, USA) was used for data quality assurance as well as variant discovery. After removing the variants with an allele frequency more than 1%, the variants shared by three affected individuals were selected. The candidate pathogenic variants were confirmed using Sanger sequencing in all family members. Primers were designed using Oligo Primer Analysis Software Version 7 (Molecular Biology

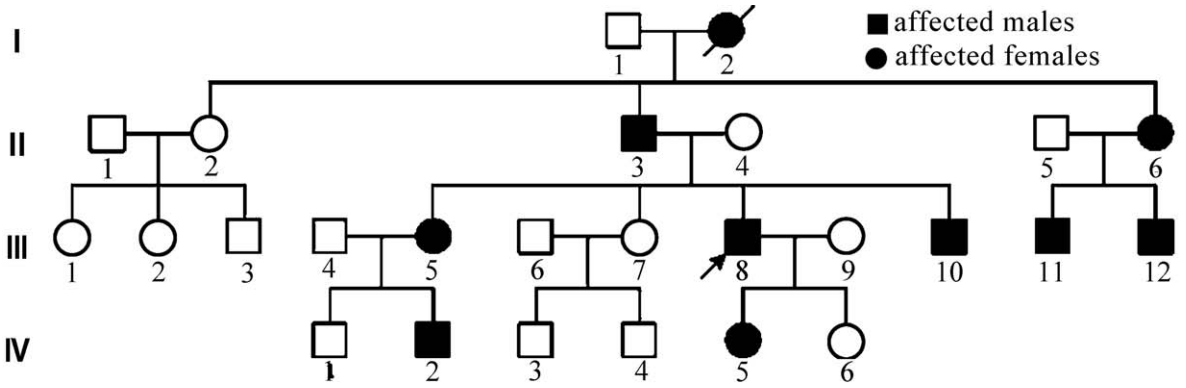

Figure 1: Pedigree of a brachydactyly and pectus carinatum family reported in this study. The arrow indicated proband (III8). The oblique line indicated dead female.

Insight, Inc., Cascade, CO, USA). Polymerase chain reaction (PCR) was performed according to the Takara protocol for Premix Taq™ (Takara Bio., Dalian, China) and purified products were run on an ABI 3730 Genetic Analyzer (Applied Biosystems, Foster City, CA, USA).

Array comparative genomic hybridization (array-CGH) analysis

The oligonucleotide CGH microarray with high probe density (SurePrint G3 Human 1x1M; Agilent) was used to analyze copy number variations (CNVs) at the whole-genome scale. The testing was performed on genomic DNA of the proband (III8). Digestion, ligation, PCR, 5-amino-propargyl-2′-deoxyuridine 5′-triphosphate coupled to Cy5 fluorescent dye (Cy5-dUTP) and Cy3-dUTP labeling, hybridization of test and reference DNA were performed according to the manufacturer's recommendations. Slides were scanned using an Agilent SureScan Microarray Scanner (Agilent), and analyzed using Agilent CytoGenomics software. Significant copy-number changes were identified by at least three consecutive aberrant probes. Reference human genome was GRCh37/hg19.

The quantitative real-time PCR assay

Quantitative real-time PCR (Q-PCR) was performed using a Rotor Gene 6000 Real-time Rotary Analyzer (QIAGEN) to validate the deletion/duplication identified by array-CGH. Q-PCR primers were designed within each flanking sequence of deletion/duplication region identified by array-CGH to validate whether the gross genomic rearrangements were co-segregated with the phenotype, and the sequences of the primers are listed in Supplementary Table 1, http://links.lww.com/CM9/A62. *C2* was used as the reference gene, and PCR amplification of target regions using SYBR® premix Ex-Taq (Takara Bio.) was performed in 20 μL PCRs with the following conditions: initial denaturation at 95°C for 5 min followed by 40 cycles, each consisting of denaturation at 95°C for 10 s, annealing at 60°C for 15 s and extension at 72°C for 20 s with a final extension at 72°C for 90 s. The relative copy number of the target sequence was calculated by the relative threshold cycle method ($2^{-\Delta\Delta Ct}$) where ΔCt = (mean Ct Target) − (mean Ct Reference) and ΔΔCt = ΔCt patient − ΔCt control. The $2^{-\Delta\Delta Ct}$ value of approximately 1.5 indicated a heterozygous duplication, and 0.5 indicated a heterozygous deletion.

Sanger sequencing of junction fragments

To precisely map the breakpoints of deletions detected by array CGH and analyze sequences of the junction fragments, gap-PCR was performed on all participants. PCR amplification of junction fragments using one pair of primer (forward 5′-TTCTTTTCCAGCACCCACAT-3′, and reverse 5′-GCATTGATTTTGGTGGGCTA-3′) was performed in 25 μL PCRs with the following conditions: an initial denaturation at 94°C for 5 min; denaturation at 94°C for 30 s, annealing at 60°C for 30 s, and extension at 72°C for 2 min, in 40 cycles, followed by a final extension for 7 min at 72°C. The amplified junction fragments were purified and run on an ABI 3730 Genetic Analyzer. The sequences were compared with the data from the UCSC Genome Browser (http://genome.ucsc.edu). Nucleotide BLAST Program (http://blast.ncbi.nlm.nih.gov/) was used to sequences aligned to check possible identical sequence between proximal and distal breakpoints.

Results

Clinical features

Multiple members of this family were affected, with the photographs of clinical features of all affected individuals shown in Figure 2. The hands and feet of affected individuals looked bulky and stocky, but the clinical features were variable in different affected individuals. All nine affected individuals had bilateral severe generalized BD of hands and feet and pectus carinatum. Two hands of the affected individual II6 (54 years old) were asymmetrical, with the left ring finger shorter than the right one. The feature of long and valgus hallux was only found in the right foot of the affected individual II6. Although the

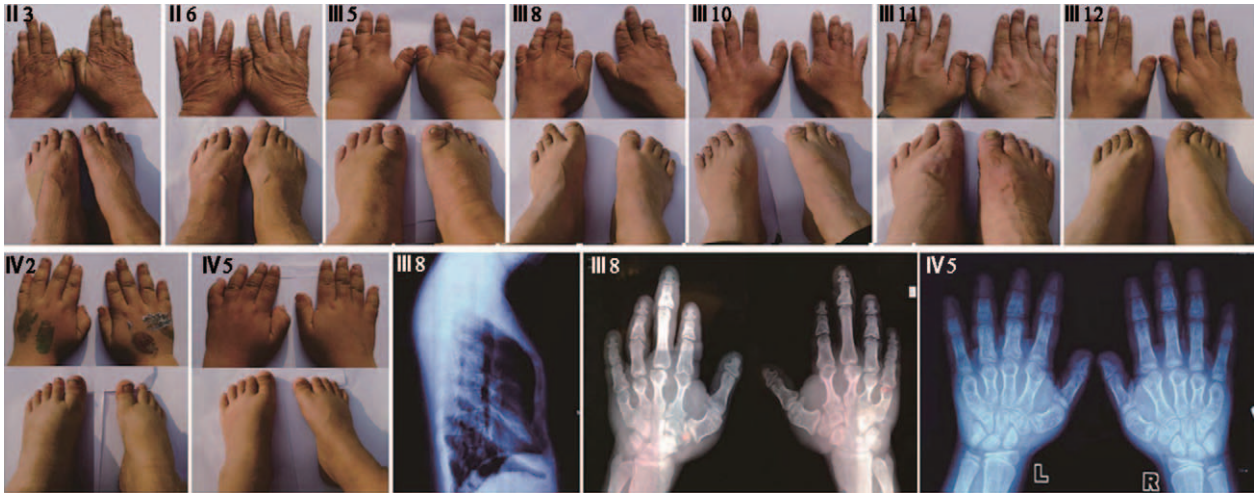

Figure 2: The clinical phenotype of this family showed that bilateral generalized brachydactyly of hands and feet and pectus carinatum. L: Left; R: Right.

affected individual III5 (36 years old) and the III8 (30 years old) both had severe and generalized BD in all finger, the middle finger of the affected individual III8 was relatively longer than the others. For the affected individual III10 (28 years old) BD of hand is most pronounced in the middle and ring fingers. The affected individual III11 (28 years old) and the III12 (24 years old) had mild BD of hands compared with the other individuals, and the shortened distal phalanges of all fingers were obvious. The younger affected individual IV2 (7 years old) and the IV5 (8 years old) had smaller hands and feet compared with normal peers and presented with generalized short and stocky hands and feet. Notably, the pectus carinatum was presented in all affected individuals. The lateral chest radiograph of individual III8 showed forward arcuate sternum [Figure 2].

Hand X-ray of individual III8 revealed that all the metacarpals of the hands were shortened, the bilateral metacarpal I was stubby and deflected to the radial side, and the metacarpals II to IV with globular ends showed as dumbbell shape. All the phalanges of the hands were also shortened, apart from the proximal phalanges of the middle finger which was relatively normal, and the irregular articular surface of ring finger proximal interphalangeal joints of the left hand was visible. The hand radiograph of individual IV5 showed that all the metacarpals of the hands were shortened as well. In addition, the epiphyses of metacarpals II to V were prematurely fused in both hands. The proximal phalanges of finger III-IV were stubby and prematurely fused of epiphyses in the left hand, whereas the anatomic form of proximal phalanges was relatively normal in the right hand. The middle phalanges of finger II-IV were stubby, and the terminal phalanges were shortened in both hands.

Body measurements revealed the affected individual with short stature. The average height of the male affected adults was shorter than 165 cm, and the female affected adults were only 150 cm. The height of individual IV5 was 115 cm, much shorter than the average level. Features of facial abnormalities, learning disabilities, mammary gland maldevelopment, dental malposition, and oligodontia were not found in this family. Laboratory testing of the bone metabolism and hormone levels indicated that the level of calcium, phosphorus, alkaline phosphatase, vitamin D3, PTH, TSH, free triiodothyronine (FT3), and free thyroxine (FT4) were normal.

Genetic analysis

Mutation detection in WES

Based on the co-segregation analysis, no strong candidate gene was found by WES in this family. The detailed information is listed in Supplementary Table 2, http://links.lww.com/CM9/A62.

Detection of array-CGH analysis and Q-PCR testing

The whole-genome array-CGH analysis in the proband (III8) revealed 13 CNVs [Supplementary Table 3, http://links.lww.com/CM9/A62] of which three were common genomic duplications and six were common genomic deletions. Four non-polymorphic CNVs (chr4:177643308-177769701 dup, 126.39 Kb; chr12: 25475995-28536312 del, 3.06 Mb; chr22: 47048713-47078331 del, 29.61 Kb; chr2: 33955377-33980856 del, 25.48 kb) were further analyzed in all family members by Q-PCR. The result of Q-PCR testing revealed that one genomic rearrangement at chr12: 25475995-28536312 (3.06 Mb) was co-segregated with the phenotype in this family [Figure 3C]. This genomic rearrangement at 12p12.1-12p11.22, presenting as a gross heterozygous deletion, encompassed 23 annotated genes, among which the *PTHLH* gene had been reported to be related to BDE, the *BHLHE41* gene had been reported to be associated with the phenotype of short sleeper (autosomal dominant inheritance, OMIM 612975), and inositol 1,4,5-trisphosphate receptor type 2 (*ITPR2*) had been reported to be associated with anhidrosis (autosomal recessive inheritance, OMIM 106190). This CNV was considered to be potentially causative because it contains a known BDE gene that might contribute to the patients' phenotype in this family. The focus was then placed on the deletion of 12p12.1-12p11.22 region.

Analysis of junction sequence

To further confirm whether the deletion was co-segregated with phenotype or not, gap-PCR was performed on genomic DNA of the family members. The result of gel electrophoresis of gap-PCR products is shown in Figure 4. Only the genomic DNA from the affected individuals was amplified, and the genomic DNA from the unaffected individuals was not amplified. Through the direct sequencing of the amplicon in nine affected family members, we identified a 3,060,317 bp deletion from chr12:25473650 to chr12:28536747. Sequence analysis found that the breakpoint junction was located in the micro-homologous sequence AT [Figure 5]. Repeat Masker analysis showed that no large segments of homologous sequences, such as L1 or Alu, existed in the 1 kb area of the breakpoint upstream/downstream.

Discussion

In this study, we report a large Chinese family with severe generalized BD of hands and feet, pectus carinatum, and short stature. The BD feature of our patients presents with severe generalized BD, all metacarpals/metatarsals were shortened, and most phalanges were involved. The phenotypes of hands and feet in this family are consistent with BDE according to the BD anatomic classification of Bell, but do not fit into any classified BDE subtypes. The feature of pectus carinatum was found in all patients, but was not reported in BD predominantly presented diseases. All the patients presented with short stature, but did not have hypertension, facial abnormalities, obesity, intellectual disability, or hormonal resistance. Genetic analysis identified a 3.06-Mb deletion (chr12:25473651-28536748) at 12p11.22-12.1, which co-segregated with the phenotype in this family. Junction sequence analysis found that micro-homologous sequence AT was located in the breakpoint junction, but no L1 or Alu was found at the breakpoint flanking sequence both upstream and downstream, suggesting that the non-homologous end joining (NHEJ) may take part in the genomic rearrangements.

Review of the previously reported 12p deletion syndromes indicated that the feature of BD was present in most reported patients, in which the deleted segment of 14 patients [Supplementary Table 4, http://links.lww.com/CM9/A62, nine patients had been reported in the literature,[6,16-22] and the other five patients reported in the DECIPHER database] overlapped with the segment of 3.06-Mb identified in our patients. Among the 14 reported patients, only three patients were not reported to have the feature of BD, including two little babies whose BD was hard to judge[19,22] and one patient who was diagnosed with osteogenesis imperfecta.[17] All the other 11 patients presented with BD of hands and/or feet, but the phenotypes were variable in different patients, ranging from shorten-

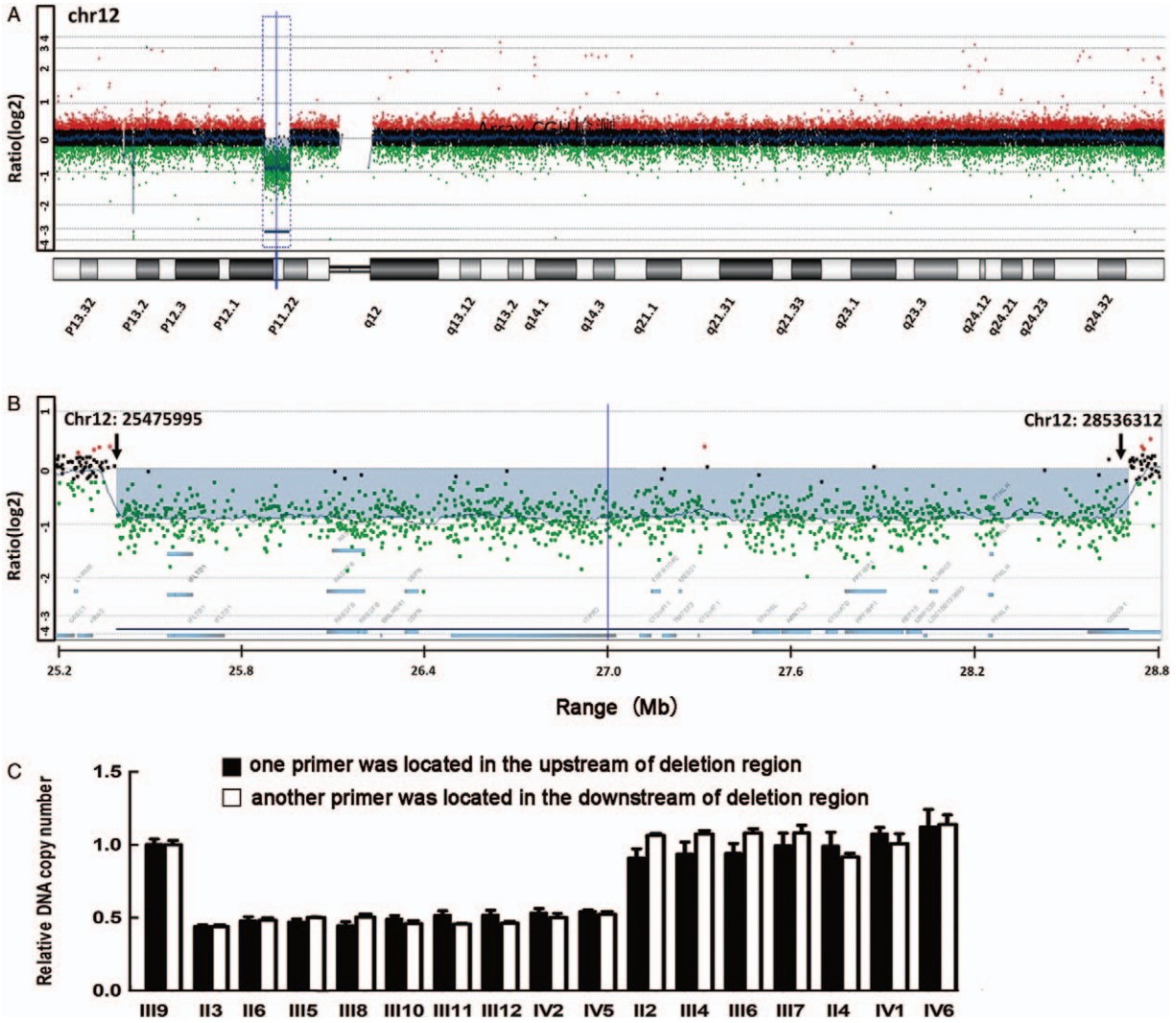

Figure 3: Array-CGH analysis showed a deletion located within the 12p11.22-p12.1 (3.06 Mb). Panel A: Array-CGH profile of chromosome 12 using the Agilent's SurePrint G3 Human 1 × 1 M. Panel B: Zoomed in version of panel A. Interstitial deletion from chr12:25475995 to chr12:28536312, the log2 ration<0.5. Panel C: Micro-deletion was confirmed by Q-PCR using Rotor Gene 6000 real-time rotary analyze. The mean values and standard deviations (error bar) for each target amplicon relative to C2, which was used as two-copy reference gene, were calculated for nine affected individuals (II3, II6, III5, III8, III10, III11, III12, IV2, and IV5) and eight unaffected individuals (II2, II4, III4, III6, III7, III9, IV1, and IV6, of which individual III9 was used as a normal individual). Q-PCR: Quantitative real-time polymerase chain reaction.

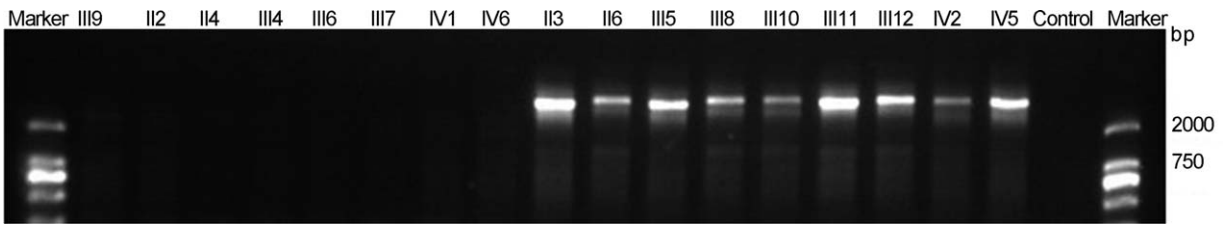

Figure 4: The agarose gel electrophoretogram of stride over breakpoint polymerase chain reaction (gap-PCR) product. An unrelated healthy individual was used as a control. The gap-PCR product was found in the lane of affected individuals (II3, II6, III5, III8, III10, III11, III12, IV2, and IV5), which was not found in the lane of unaffected individuals (III9, II2, II4, III4, III6, III7, IV1, and IV6) and unrelated healthy individual.

ing of the individual metacarpals and/or phalanges to shortening of all bones in the hands and feet. Most of them (12/14) had the feature of short stature, whereas the patients in our study presented with short stature. Some of them (13/14) with the larger deleted region than we reported patient's had intellectual disability, facial dysmorphism or developmental delay, but these features were not found in our patients, which made us speculate that additional deleted genes in these cases might be responsible for these phenotypes. However, Klopocki *et al* reported[6] that patients with a smaller deleted region than the 3.06 Mb interval also had the feature of intellectual disability. So, other reasons such as epigenetic modification might contribute to this phenotype.

Within the smallest overlapped region of reported 12p deletion, *PTHLH* was the first reported pathogenic gene associated with BDE2. Maass *et al*[23] identified a balanced t(8;12)(q13;p11.2) translocation with breakpoints upstream of *PTHLH* on chromosome 12p11.2, leading to BDE. Later, Klopocki *et al*[6] identified loss of function mutations of *PTHLH* to be associated with BDE with short stature. Recently, other families and sporadic patients with BDE and short statures carrying point mutations and small deletions of *PTHLH* have been reported in the literatures.[7-9,24,25] Based on the described findings above, we concluded that the 3.06 Mb deletion identified in this study was responsible for the abnormal clinical manifestation in the family reported in our study, and the features of severe generalized BD of hands and feet and short stature were mainly caused by haploinsufficiency of *PTHLH* located within this deleted region.

The feature of pectus carinatum was not found in the previously reported patients of 12p deletion syndromes. However, the feature of chest deformity, such as asymmetric thorax, broad thorax, and asphyxiating thoracic dystrophy, were found in four reported patients.[16-19] The features of widespread abnormalities of endochondral bone development and the narrow bell-shaped thoracic cage were found in homozygous mice with *Pthlh* null mutation, although the heterozygous mice had no apparently distinct phenotype when compared with their wild-type littermates.[26] These results suggested that *PTHLH* played an important role in the normal development of thorax. The chest deformity of our reported family and some other patients with 12p deletion[16-19] was a milder presentation without respiratory symptoms. We concluded that the feature of chest deformity was also mainly caused by haploinsufficiency of *PTHLH*. Different combinations of modifier genes could potentially explain the phenotypic variations.

PTHLH is an important regulator of endochondral bone development. During skeletal development, *PTHLH* is expressed in perichondrial cells and chondrocytes at the end of growing bone.[27] Its produces parathyroid-hormone-related protein (PTHrP) to bind the PTH/PTHrP receptor resulting in Gs activation, which in turn promotes chondrocytes proliferating and undifferentiation in combination with the process mediated by suppression of p57 and Runx2 and phosphorylation of the transcription factor SOX9, thereby increasing the pool of proliferating chondrocytes.[28] The synthesis of PTHrP is regulated by IHH, to form a feedback loop that regulates the chondrocytes proliferating, hypertrophic differentiation and endochondral bone development.[29] Bone lengthening is caused by an increase in chondrocytes number, synthesis of chondrocytes matrix and substantial enlargement of chondrocytes that occurs during hypertrophy. If one of the pathways abovementioned is abnormal, it will lead to dysplasia and growth disorder of bone. All reported patients with mutations and/or micro-deletions of *PTHLH* presented with complete penetrance of the BDE phenotype, but showed a high degree of phenotypic variability. Even in the presence of point mutations of *PTHLH*, some patients presented with severe and generalized BD,[7] others only presented with single metacarpal shortened.[9] This characteristic of high variable expressivity may be a feature of *PTHLH*-related BDE, which may easily lead to misdiagnosis. Therefore, genetic testing is very important for an accurate diagnosis of *PTHLH*-related BDE.

In addition, PTHrP is expressed and secreted by a variety of tissues[30] except cartilaginous tissue and plays an important role in the developmental stages of mammary glands, hair follicles, and teeth.[31] The ectodermal dysplastic phenotypes, such as the absence of mammary development, failure of tooth eruption, and abnormalities of the skin, were found in rescued PTHrP(−/−) mice.[32,33] Some reported patients[6,9,16-18] had the features of dental anomalies, such as dental malposition, oligodontia, and tooth eruption problem, and small breasts in two patients.[9] However, in the family reported in our study,

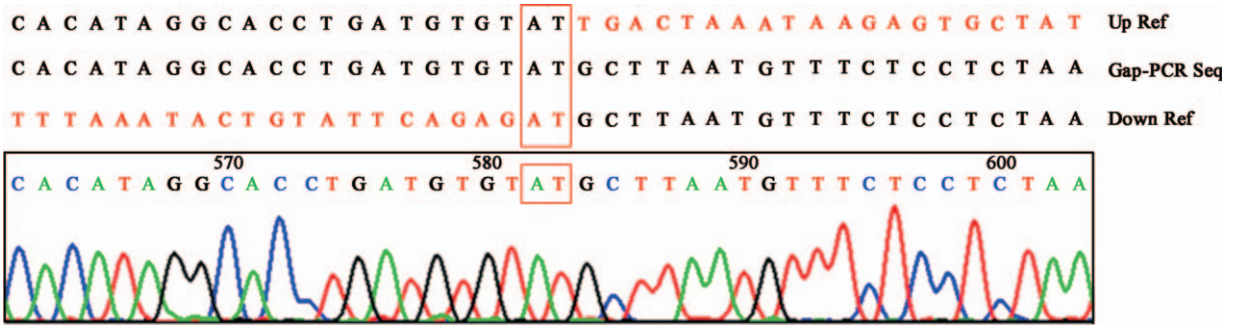

Figure 5: The sequencing result of the stride over breakpoint polymerase chain reaction (gap-PCR) product. The nucleotide of micro-homology AT (2 bp) was marked by a red box. The upstream micro-homology AT was located in chr12:25473648-25473649, and the downstream micro-homology AT located in chr12:28536746-28536747.

no patient was observed to have the feature of dental anomalies and mammary gland maldevelopment. These indicate that *PTHLH* variation has a broad spectrum of the syndrome in humans.

The 3.06-Mb genomic rearrangement identified in this family encompassed 23 annotated genes, for which gene functions were reviewed [Supplementary Table 5, http://links.lww.com/CM9/A62]. We found that no genes other than *PTHLH* have been reported to be associated with bone development. In the deletion region, *BHLHE41* and *ITPR2* had been reported to be related to the short sleeper and anhidrosis, respectively. However, patients with short sleeper carried a p.P385R heterozygous mutation of *BHLHE41*, leading to the phenotype by this dominant negative mutation,[34] whereas anhidrosis caused by *ITPR2* mutation is inherited in an autosomal recessive manner.[35] Our reported family with one copy of *BHLHE41* and *ITPR2* deletion did not show the features of short sleeper and anhidrosis, consistent with the findings above mentioned. Whether the other genes within the deletion region contribute to phenotype needs further study.

In this study, we used WES and Array-CGH to detect the pathogenic variation of one Chinese family with unclassified BDE, and a 3.06-Mb deletion of 12p12.1-12p11.22 was co-segregated with the phenotype in this family. In the deletion region, *PTHLH* was the only one reported pathogenic gene associated with BDE. Review of the previously reported patients, we found that *PTHLH*-related BDE has the high variable expressivity and some patients are also accompanied by ectodermal dysplasia phenotype. The patients reported in our study also presented with pectus carinatum which was not found in other patients reported in the literature. Our study has expanded the knowledge on the phenotypic presentation of *PTHLH* variation; however, our study did not explain the reason for the variable expressivity. The variation of interaction gene in the developmental pathway and epigenetic modification may contribute to *PTHLH*-related disease variable expressivity. In conclusion, we report a family with a combination of BDE and pectus carinatum. The 3.06-Mb deletion of 12p12.1-12p11.22 co-segregated with the phenotype in this family and the *PTHLH* located in this region are the main candidate pathogenic gene.

Funding

This work was supported by grants from the National Key Research and Development Program of China (No. 2016YFC0905100), the CAMS Innovation Fund for Medical Sciences (CIFMS; No. 2016-I2M-1-002), Medical Science and Technology Key Projects of Henan Province (No. 201601019), and Technology Key Projects of Henan Province Health Bureau (No. 182102310170).

Conflicts of interest

None.

References

1. Mundlos S. The brachydactylies: a molecular disease family. Clin Genet 2009;76:123–136. doi: 10.1111/j.1399-0004.2009.01238.x.
2. Bell J. On brachydactyly and symphalangism. In: Penrose LS. Treasury of Human Inheritance. London: Cambridge University Press; 1951;1–31.
3. Hertzog KP. Brachydactyly and pseudo-pseudohypoparathyroidism. Acta Genet Med Gemellol (Roma) 1968;17:428–438.
4. Johnson D, Kan SH, Oldridge M, Trembath RC, Roche P, Esnouf RM, *et al*. Missense mutations in the homeodomain of HOXD13 are associated with brachydactyly types D and E. Am J Hum Genet 2003;72:984–997. doi.org/10.1086/374721.
5. Jamsheer A, Sowinska A, Kaczmarek L, Latos-Bielenska A. Isolated brachydactyly type E caused by a HOXD13 nonsense mutation: a case report. BMC Med Genet 2012;13:4. doi: 10.1186/1471-2350-13-4.
6. Klopocki E, Hennig BP, Dathe K, Koll R, de Ravel T, Baten E, *et al*. Deletion and point mutations of PTHLH cause brachydactyly type E. Am J Hum Genet 2010;86:434–439. doi: 10.1016/j.ajhg.2010.01.023.
7. Wang J, Wang Z, An Y, Wu C, Xu Y, Fu Q, *et al*. Exome sequencing reveals a novel PTHLH mutation in a Chinese pedigree with brachydactyly type E and short stature. Clin Chim Acta 2015;446:9–14. doi: 10.1016/j.cca.2015.03.019.
8. Jamsheer A, Sowinska-Seidler A, Olech EM, Socha M, Kozlowski K, Pyrkosz A, *et al*. Variable expressivity of the phenotype in two families with brachydactyly type E, craniofacial dysmorphism, short stature and delayed bone age caused by novel heterozygous mutations in the PTHLH gene. J Hum Genet 2016;61:457–461. doi: 10.1038/jhg.2015.172.
9. Thomas-Teinturier C, Pereda A, Garin I, Diez-Lopez I, Linglart A, Silve C, *et al*. Report of two novel mutations in PTHLH associated with brachydactyly type E and literature review. Am J Med Genet A 2016;170:734–742. doi: 10.1002/ajmg.a.37490.
10. Schuster H, Wienker TE, Bahring S, Bilginturan N, Toka HR, Neitzel H, *et al*. Severe autosomal dominant hypertension and brachydactyly in a unique Turkish kindred maps to human chromosome 12. Nat Genet 1996;13:98–100. doi: 10.1038/ng0596-98.
11. Toka HR, Bahring S, Chitayat D, Melby JC, Whitehead R, Jeschke E, *et al*. Families with autosomal dominant brachydactyly type E, short stature, and severe hypertension. Ann Intern Med 1998;129:204–208. doi: 10.7326/0003-4819-129-3-199808010-00008.
12. Maass PG, Aydin A, Luft FC, Schachterle C, Weise A, Stricker S, *et al*. PDE3A mutations cause autosomal dominant hypertension with brachydactyly. Nat Genet 2015;47:647–653. doi: 10.1038/ng.3302.
13. Bastepe M, Juppner H. GNAS locus and pseudohypoparathyroidism. Horm Res 2005;63:65–74. doi: 10.1159/000083895.
14. Linglart A, Fryssira H, Hiort O, Holterhus PM, Perez de Nanclares G, Argente J, *et al*. PRKAR1A and PDE4D mutations cause acrodysostosis but two distinct syndromes with or without GPCR-signaling hormone resistance. J Clin Endocrinol Metab 2012;97:E2328–E2338. doi: 10.1210/jc.2012-2326.
15. Lynch DC, Dyment DA, Huang L, Nikkel SM, Lacombe D, Campeau PM, *et al*. Identification of novel mutations confirms PDE4D as a major gene causing acrodysostosis. Hum Mutat 2013;34:97–102. doi: 10doi: 10.1002/humu.22222.
16. Magnelli NC, Therman E. Partial 12p deletion: a cause for a mental retardation, multiple congenital abnormality syndrome. J Med Genet 1975;12:105–108. doi: 10.1136/jmg.12.1.105.
17. Orye E, Craen M. Short arm deletion of chromosome 12: report of two new cases. Humangenetik 1975;28:335–342.
18. Nagai T, Nishimura G, Kato R, Hasegawa T, Ohashi H, Fukushima Y. Del(12)(p11.21p12.2) associated with an asphyxiating thoracic dystrophy or chondroectodermal dysplasia-like syndrome. Am J Med Genet 1995;55:16–18. doi: 10.1002/ajmg.1320550106.
19. Glaser B, Rossier E, Barbi G, Chiaie LD, Blank C, Vogel W, *et al*. Molecular cytogenetic analysis of a constitutional de novo interstitial deletion of chromosome 12p in a boy with developmental delay and congenital anomalies. Am J Med Genet A 2003;116A:66–70. doi: 10.1002/ajmg.a.10878.
20. Lu HY, Cui YX, Shi YC, Xia XY, Liang Q, Yao B, *et al*. A girl with distinctive features of borderline high blood pressure, short stature, characteristic brachydactyly, and 11.47 Mb deletion in 12p11-21-12p12. 2 by oligonucleotide array CGH. Am J Med Genet A 2009;149A:2321–2323. doi: 10.1002/ajmg.a.33030.
21. Soysal Y, Vermeesch J, Davani NA, Hekimler K, Imirzalioglu N. A 10.46 Mb 12p11.1-12.1 interstitial deletion coincident with a 0.19 Mb NRXN1 deletion detected by array CGH in a girl with scoliosis and autism. Am J Med Genet A 2011;155A:1745–1752. doi: 10.1002/ajmg.a.34101.

22. Hoppe A, Heinemeyer J, Klopocki E, Graul-Neumann LM, Spors B, Bittigau P, *et al*. Interstitial 12p deletion involving more than 40 genes in a patient with postnatal microcephaly, psychomotor delay, optic nerve atrophy, and facial dysmorphism. Meta Gene 2014;2:72–82. doi: 10.1016/j.mgene.2013.10.014.
23. Maass PG, Wirth J, Aydin A, Rump A, Stricker S, Tinschert S, *et al*. A cis-regulatory site downregulates PTHLH in translocation t(8;12)(q13;p11.2) and leads to Brachydactyly Type E. Hum Mol Genet 2010;19:848–860. doi: 10.1093/hmg/ddp553.
24. Pereda A, Garzon-Lorenzo L, Garin I, Cruz-Rojo J, Sanchez Del Pozo J, Perez de Nanclares G. The p.R56 mutation in PTHLH causes variable brachydactyly type E. Am J Med Genet A 2017;173:816–819. doi: 10.1002/ajmg.a.38067.
25. Bae J, Choi HS, Park SY, Lee DE, Lee S. Novel mutation in PTHLH related to brachydactyly type E2 initially confused with unclassical pseudopseudohypoparathyroidism. Endocrinol Metab (Seoul) 2018;33:252–259. doi: 10.3803/EnM.2018.33.2.252.
26. Karaplis AC, Luz A, Glowacki J, Bronson RT, Tybulewicz VL, Kronenberg HM, *et al*. Lethal skeletal dysplasia from targeted disruption of the parathyroid hormone-related peptide gene. Genes Dev 1994;8:277–289. doi: 10.1101/gad.8.3.277.
27. Lee K, Deeds JD, Segre GV. Expression of parathyroid hormone-related peptide and its receptor messenger ribonucleic acids during fetal development of rats. Endocrinology 1995;136:453–463. doi: 10.1210/endo.136.2.7835276.
28. Kronenberg HM. PTHrP and skeletal development. Ann N Y Acad Sci 2006;1068:1–13. doi: 10.1196/annals.1346.002.
29. van Donkelaar CC, Huiskes R. The PTHrP-Ihh feedback loop in the embryonic growth plate allows PTHrP to control hypertrophy and Ihh to regulate proliferation. Biomech Model Mechanobiol 2007;6:55–62. doi: 10.1007/s10237-006-0035-0.
30. de Papp AE, Stewart AF. Parathyroid hormone-related protein a peptide of diverse physiologic functions. Trends Endocrinol Metab 1993;4:181–187. doi: org/10.1016/1043-2760(93)90114-T.
31. McCauley LK, Martin TJ. Twenty-five years of PTHrP progress: from cancer hormone to multifunctional cytokine. J Bone Miner Res 2012;27:1231–1239. doi: 10.1002/jbmr.1617.
32. Schipani E, Lanske B, Hunzelman J, Luz A, Kovacs CS, Lee K, *et al*. Targeted expression of constitutively active receptors for parathyroid hormone and parathyroid hormone-related peptide delays endochondral bone formation and rescues mice that lack parathyroid hormone-related peptide. Proc Natl Acad Sci U S A 1997;94:13689–13694. doi: 10.1073/pnas.94.25.13689.
33. Wysolmerski JJ, Philbrick WM, Dunbar ME, Lanske B, Kronenberg H, Broadus AE. Rescue of the parathyroid hormone-related protein knockout mouse demonstrates that parathyroid hormone-related protein is essential for mammary gland development. Development 1998;125:1285–1294.
34. He Y, Jones CR, Fujiki N, Xu Y, Guo B, Holder JL Jr, *et al*. The transcriptional repressor DEC2 regulates sleep length in mammals. Science 2009;325:866–870. doi: 10.1126/science.1174443.
35. Klar J, Hisatsune C, Baig SM, Tariq M, Johansson AC, Rasool M, *et al*. Abolished InsP3R2 function inhibits sweat secretion in both humans and mice. J Clin Invest 2014;124:4773–4780. doi: 10.1172/JCI70720.

How to cite this article: Huang J, Liu HY, Wang RR, Xiao H, Wu D, Li T, Jiang YH, Zhang X. A 3.06-Mb interstitial deletion on 12p11.22-12.1 caused brachydactyly type E combined with pectus carinatum. Chin Med J 2019;132:1681–1688. doi: 10.1097/CM9.0000000000000327